arXiv:1409.5922v1 [cs.DM] 20 Sep 2014

Automated Discharging Arguments for Density Problems in Grids (Extended Abstract*)

Derrick Stolee
Department of Computer Science
Department of Mathematics
Iowa State University
dstolee@iastate.edu

September 23, 2014

Abstract

Discharging arguments demonstrate a connection between local structure and global averages. This makes it an effective tool for proving lower bounds on the density of special sets in infinite grids. However, the minimum density of an identifying code in the hexagonal grid remains open, with an upper bound of $\frac{3}{7} \approx 0.428571$ and a lower bound of $\frac{5}{12} \approx 0.416666$. We present a new, experimental framework for producing discharging arguments using an algorithm. This algorithm replaces the lengthy case analysis of human-written discharging arguments with a linear program that produces the *best possible* lower bound using the specified set of discharging rules. We use this framework to present a lower bound of $\frac{23}{55} \approx 0.418181$ on the density of an identifying code in the hexagonal grid, and also find several sharp lower bounds for variations on identifying codes in the hexagonal, square, and triangular grids.

*Pages 2-11 of this PDF contain the extended abstract, with some figures and tables appearing in appendices (pp. 14-17).

1 Introduction

The discharging method is a well-known technique in discrete mathematics, especially due to its use in the computer-assisted proofs of the Four Color Theorem [1,2,30]. Since that first incredible achievement, almost all other discharging proofs have been done manually. Applications of discharging include coloring planar graphs [6], density problems in grids [7,8], and structural problems on circulant graphs [11]. Despite its wide use, producing an effective discharging argument is very challenging and the proofs become weighted down by a lengthy case analysis. We present an experimental method for automatically producing discharging arguments and apply this method to prove lower bounds on the density of sets in infinite grids.

A *plane grid* is an infinite graph embedded in the plane. We will consider three plane grids: the hexagonal grid, the square grid, and the triangular grid, as shown in Figure 1. These grids model the structure of a wireless sensor network where the nodes are placed in a rigid lattice, as would be typical for use in a field for drought monitoring [9]. Due the low cost of wireless sensor nodes, these networks can be so large that the boundary of the network is a small portion of the entire network, so using an infinite grid is an effective way to approximate the network. Karpovsky, Chakrabarty, and Levitin [21] considered the problem of detecting faults in such a network and defined an *identifying code* to be a set X of vertices in the grid where the intersection of X with the closed neighborhood of each vertex is distinct. If $N(v)$ is the set of vertices adjacent to v, then the closed neighborhood $N[v]$ is the set $N(v) \cup \{v\}$. Thus an identifying code X in a grid G satisfies

$$N[v] \cap X \neq \varnothing, \forall v \in V(G), \qquad \text{and} \qquad N[v] \cap X \neq N[u] \cap X, \forall u, v \in V(G), u \neq v.$$

An identifying code exists in a graph G if and only if there are no *twins* (distinct vertices u, v where $N[u] = N[v]$) since using the entire vertex set can identify all vertices. The interesting problem is to determine the *smallest* identifying code in G, to minimize the cost of placing fault-detection devices on the nodes representing elements of the code.

In an infinite grid, any identifying code will be infinite, so we need a notion of density instead of size. For a vertex v, let $B_r(v)$ be the set of vertices within distance r of v in G. The *density* of a set $X \subseteq V(G)$, denoted $\delta(G)$, is defined as a limit of the proportion of elements of X in the ball of radius r, as r grows.

$$\delta(X) = \limsup_{r \to \infty} \frac{|B_r(v) \cap X|}{|B_r(v)|} \text{ for some vertex } v \in V(G).$$

Cohen *et al.* [5] demonstrated an identifying code in the hexagonal grid of density $\frac{3}{7}$, and Cukierman and Yu [8] found several other constructions of this density. However, lower bounds on the optimal density have not reached this upper bound, despite several attempts [5, 7, 8, 21]. Table 1 summarizes these efforts, including the new lower bound demonstrated in this paper.

Theorem 1. *If X is an identifying code in the hexagonal grid, then $\delta(X) \geq \frac{23}{55} = 0.4\overline{18}$.*

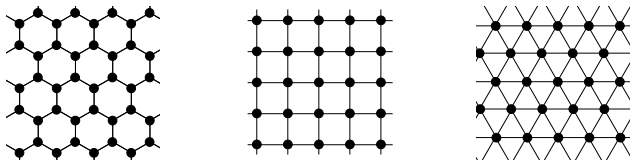

(a) Hexagonal Grid (b) Square Grid (c) Triangular Grid

Figure 1: Examples of plane grids.

Karpovsky, Chakrabarty, and Levitin [21]	$0.400000 = \frac{2}{5} \leq \delta \leq \frac{1}{2} = 0.500000$
Cohen, Honkala, Lobstein, and Zémor [5]	$0.410256 \approx \frac{16}{39} \leq \delta \leq \frac{3}{7} \approx 0.428571$
Cranston and Yu [7]	$0.413793 \approx \frac{12}{29} \leq \delta$
Cukierman and Yu [8]	$0.416666 \approx \frac{5}{12} \leq \delta$
New Lower Bound	$0.418182 \approx \frac{23}{55} \leq \delta$

Table 1: Existing bounds on δ, the minimum density of an identifying code in the hexagonal grid.

We prove Theorem 1 using a new computer-automated method for constructing discharging arguments. Due to the generality of the method and the modular nature of the implementation, the method also demonstrates lower bounds for other grids and for other variants on identifying codes. Thus, several sharp lower bounds are proven for these variants in the hexagonal, square, and triangular grids, which were major theorems of previous work [3, 16, 21, 22, 31, 33].

Our main contribution is the development of this new computational approach to producing discharging arguments. In Section 3, we discuss the structure of our discharging arguments. A recent survey by Cranston and West [6] includes a more general perspective, but focuses more on coloring planar graphs. Briefly, discharging arguments all feature three main steps: (1) assigning initial charge, (2) distributing charge according to certain discharging rules, and (3) verifying that all objects have the goal amount of charge. The most novel contribution of this new framework is that steps (2) and (3) are done in opposite order. By using a combinatorial generation algorithm, we enumerate every possible way that the discharging rules can interact on a single object and create a linear program based on those interactions. Every feasible solution corresponds to a correct discharging argument, and an optimal solution provides the largest lower bound possible using that set of rules. This pairing of combinatorial generation and linear programming is similar to the use of generating and solving a semidefinite program in Razborov's flag algebra method [27], which has gained significant attention in recent years (see Razborov's survey [28]).

The purpose of this extended abstract is to demonstrate how a custom computer algorithm can produce a discharging argument using minimal human interaction. We name our method *ADAGE* for "Automated Discharging Arguments using GEneration," and a specific proof using the framework is an *adage*. While an adage is a short saying that conveys a general truth, an adage proof has a very short description while the computer handles the significant case analysis. In Section 2 we discuss the important properties of the plane grids in more detail, followed by a definition of a *configuration* and *forbidden configuration*. In Section 3 we set up the discharging argument, demonstrate how it is linked to the density of a set X, and discuss the structure of discharging rules. The most crucial step is discussed in Section 4, where a linear program is built to satisfy the assertions of the discharging argument. Section 5 defines several variations on an identifying code, and the results on these variations are listed in Table 5. Appendices A and B list several options for possible discharging rules in the three grids and the lower bounds demonstrated by the adage proofs using those rules.

2 Grids, Density, and Configurations

For a grid G, we use $V(G)$ to denote the set of vertices in G and $F(G)$ to denote the set of faces in G. We shall use standard graph theory terminology (see West [36]) to treat a grid G as an infinite plane graph with vertex set $V(G)$, edge set $E(G)$, and face set $F(G)$.

The grids G have an automorphism group as graphs, but we will restrict the automorphisms to be affine linear maps on the plane with determinant 1. Specifically, we allow rigid motions that are translations and

rotations, but do not allow reflection (as such maps would have determinant -1). We make this restriction based on intuition since previous discharging arguments in grids have made use of distinguishing between clockwise and counter-clockwise arrangements, which would be lost if we allowed reflection. Under these automorphisms, all three grids are vertex- and face-transitive. If we did not allow rotation, then the hexagonal grid would not be vertex-transitive and the triangular grid would not be face-transitive.

For a vertex $v \in V(G)$ and an integer $r \geq 0$, the *ball of radius r around v* is the set of vertices within distance r of v and is denoted by $B_r(v)$. The *faces within distance r of v* is the set of faces incident to vertices in $B_{r-1}(v)$ and is denoted by $F_r(v)$. For a face $f \in F(G)$, define $B_r(f)$ to be the vertices v where $f \in B_r(v)$ and $F_r(f)$ to be the faces incident to vertices in $B_{r-1}(f)$.

A grid is *amenable* if the maximum degree of a vertex in G is finite, the maximum length of a face in G is finite, and $\lim_{r\to\infty} \frac{|B_{r+d}(v)\setminus B_r(v)|}{|B_r(v)|} = 0$ for all finite values $d \geq 0$. Amenable grids have the property that the boundary of a ball is a vanishing proportion of the volume of the ball as the radius of the ball grows. Using this basic property, it is not difficult to make the following observation.

Observation 2. *Let G be an amenable plane grid. Then, for $u, v \in V(G)$, $\lim_{r\to\infty} \frac{|B_r(u)\cap B_r(v)|}{|B_r(u)\cup B_r(v)|} = 1$, and hence for any set $X \subseteq V(G)$,*

$$\limsup_{r\to\infty} \frac{|B_r(u) \cap X|}{|B_r(u)|} = \limsup_{r\to\infty} \frac{|B_r(v) \cap X|}{|B_r(v)|}.$$

By this observation, we can define one vertex in $V(G)$ as the "zero vertex," denoted by v_0, and define the *density* of a set $X \subseteq V(G)$ to be the limit $\delta(X) = \limsup_{r\to\infty} \frac{|B_r(v_0)\cap X|}{|B_r(v_0)|}$. We also define one face in $F(G)$ as the "zero face" denoted by f_0.

A *configuration* is a tuple (V, S_0, S_1, F) where V is a finite set of vertices in $V(G)$, S_0 and S_1 are disjoint subsets of V, and F is a finite set of faces in $F(G)$. We call S_1 the *elements* and S_0 the *nonelements*. While we require that $S_0 \cap S_1 = \varnothing$, we do not require that $S_0 \cup S_1 = V$. Vertices in $V \setminus (S_0 \cup S_1)$ are considered *undetermined vertices*. Frequently, we will denote a configuration by C and refer to the entries of the tuple (V, S_0, S_1, F) by $V(C)$, $S_0(C)$, $S_1(C)$, and $F(C)$. The automorphism group of G naturally acts on configurations to produce a notion of isomorphism between configurations.

Such a configuration C represents a finite induced subgraph of the grid G and its planar dual G^*, as well as some information about X on that induced subgraph. Specifically, a configuration C is *embedded* in X if $S_1(C) \subseteq X$, and $S_0(C) \subseteq V(G) \setminus X$. Further, C is *embeddable* in X if there exists a configuration C' isomorphic to C such that C' is embedded in X.

Many families of subsets of $V(G)$, such as identifying codes, can be defined in terms of *forbidden configurations*. Given a collection $\mathcal{F} = \{C_1, \ldots, C_k\}$ of configurations, the family $\mathrm{forb}(\mathcal{F})$ consists of sets $X \subset V(G)$ where for every $C_i \in \mathcal{F}$, the configuration C_i is not embeddable in the set X. For a single configuration C, we use $\mathrm{forb}(C)$ to denote $\mathrm{forb}(\{C\})$.

For example, a *dominating set* is a set $X \subseteq V(G)$ such that $N[v] \cap X \neq \varnothing$ for all vertices $v \in V(G)$. If $v \in V(G)$ and C is the configuration with $V(C) = S_0(C) = N[v]$, then $\mathrm{forb}(C)$ is the family of dominating sets in G. Observe that for the family $\mathcal{F}$ of configurations in Figure 2, $\mathrm{forb}(\mathcal{F})$ is the family of identifying codes in the hexagonal grid.

For a family $\mathcal{F} = \{C_1, \ldots, C_k\}$ of forbidden configurations and a configuration C where $S_0(C) = S_1(C) = \varnothing$, we say that a configuration C' is an $\mathcal{F}$-realization of C if $V(C') = V(C)$, $S_0(C') \cup S_1(C') = V(C')$, and C' does not contain any configuration $C_i \in \mathcal{F}$. It is not difficult to generate all $\mathcal{F}$-realizations of a configuration C up to isomorphism using standard techniques. If $\mathcal{F} = \varnothing$, then there are $2^{|V(C)|}$ realizations of C, and possibly fewer when $\mathcal{F} \neq \varnothing$.

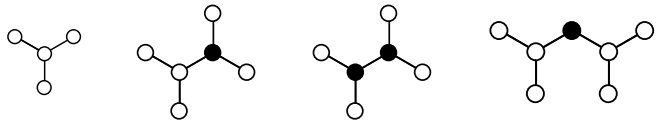

Figure 2: Forbidden configurations for identifying codes in the hexagonal grid.

We will use this method of generating $\mathcal{F}$-realizations of a configuration C to examine all cases of how an embedding of C in the grid G can intersect a set X. But first, we must discuss the structure of our discharging argument.

3 Charge Assignment and Discharging Rules

For our discharging argument, we will consider vertices and faces of G to be *chargeable objects* in that we will associate them with a numerical value, called a *charge*. We assign a charge function $\mu\colon V(G) \to \mathbb{R}$ on the vertices of G and a charge function $\nu\colon F(G) \to \mathbb{R}$ on the faces of G. These functions are based on the positions of the elements in a set $X \subseteq V(G)$: for every vertex $v \in V(G)$, $\mu(v) = \begin{cases} 1 & v \in C, \\ 0 & v \notin C \end{cases}$, and for every face $f \in F(G)$, let $\nu(f) = 0$. Observe that $\sum_{v \in B_r(v_0)} \mu(v) + \sum_{f \in F_r(v_0)} \nu(f) = |X \cap B_r(v_0)|$ and hence

$$\delta(X) = \limsup_{r\to\infty} \frac{|X \cap B_r(v_0)|}{|B_r(v_0)|} = \limsup_{r\to\infty} \frac{\sum_{v \in B_r(v_0)} \mu(v) + \sum_{f \in F_r(v_0)} \nu(f)}{|B_r(v_0)|}.$$

A *discharging function* is a function $D_X\colon (V(G) \cup F(G)) \times (V(G) \cup F(G)) \to \mathbb{R}$ where $D_X(x, y) = -D_X(y, x)$ for all $x, y \in V(G) \cup F(G)$. Specifically, we can say that for two chargeable objects $x, y \in V(G) \cup F(G)$, the value $D_X(x, y)$ is the amount of charge to *exchange from x to y*. Given a discharging function D_X, we define the resulting charge functions $\mu'\colon V(G) \to \mathbb{R}$ and $\nu'\colon F(G) \to \mathbb{R}$ as follows:

$$\mu'(v) = \mu(v) + \sum_{u \in V(G)} D_X(u, v) + \sum_{g \in F(G)} D_X(g, v).$$
$$\nu'(v) = \nu(f) + \sum_{u \in V(G)} D_X(u, f) + \sum_{g \in F(G)} D_X(g, f).$$

For values $c, d > 0$, we say that D_X is (c, d)-*local* if $|D_X(x, y)| \leq c$ always, and $D_X(x, y) = 0$ whenever the distance between x and y in G exceeds d. If a discharging function D_X is (c, d)-local, then as a ball grows, the change in the total charge between the initial charge functions μ, ν and the final charge functions μ', ν' are negligible compared to the size of the ball.

Our main assertion for a "good" discharging function is that the resulting charge functions satisfy $\mu'(v) \geq w$ and $\nu'(f) \geq 0$ for all vertices $v \in V(G)$ and faces $f \in F(G)$. Roughly, this means that the initial charge on the vertices was "spread out" evenly so that every vertex has at least w units of charge, and the faces did not contribute any positive charge to the vertices and instead were simply "messengers" of charge. In the hexagonal grid, passing charge between vertices and faces can be particularly effective, since a face is incident to three antipodal pairs of vertices.

We make this assertion of a good discharging function concrete in the following theorem.

Theorem 3. *Let G be an amenable grid. Let $X \subseteq V(G)$, $c, d, w \geq 0$, and let D_X be a (c, d)-local discharging function. Define the charge functions μ, μ', ν, ν' by the discharging process using X and D_X. If $\mu'(v) \geq w$ for all $v \in V(G)$ and $\nu'(f) \geq 0$ for all $f \in F(G)$, then $\delta(X) \geq w$.*

Proof. By Observation 2, we can select the zero vertex v_0 and zero face f_0 such that $|B_d(v_0)| = \max\{|B_d(v)| : v \in V(G)\}$ and $|F_d(f_0)| = \max\{|F_d(f)| : f \in F(G)\}$.

Recall that by the definitions of μ and ν,

$$\delta(X) = \limsup_{r\to\infty} \frac{|X \cap B_r(v_0)|}{|B_r(v_0)|} = \limsup_{r\to\infty} \frac{\sum_{v\in B_r(v_0)} \mu(v) + \sum_{f\in F_r(v_0)} \nu(f)}{|B_r(v_0)|} \tag{1}$$

By hypothesis,

$$\limsup_{r\to\infty} \frac{\sum_{v\in B_r(v_0)} \mu'(v) + \sum_{f\in F_r(v_0)} \nu'(f)}{|B_r(v_0)|} \geq \limsup_{r\to\infty} \frac{\sum_{v\in B_r(v_0)} w + \sum_{f\in F_r(v_0)} 0}{|B_r(v_0)|} = w. \tag{2}$$

Our goal is to prove that the limit at the end of (1) and the limit at the beginning of (2) are equal, thereby showing that $\delta(X) \geq w$.

Using the definition of μ' and ν' and the fact that D_X is (c,d)-local, we find that the absolute difference $\left|\sum_{v\in B_r(v_0)} [\mu'(v) - \mu(v)] + \sum_{f\in F_r(v_0)} [\nu'(f) - \nu(f)]\right|$ is equal to the magnitude of the charge that D_X exchanges across the boundaries of $B_r(v_0)$ and $F_r(f)$:

$$\begin{aligned}
&\left|\sum_{v\in B_r(v_0)} \left[\sum_{u\notin B_r(v_0)} D_X(u,v) + \sum_{g\notin F_r(v_0)} D_X(g,v)\right] + \sum_{f\in F_r(v_0)} \left[\sum_{u\notin B_r(v_0)} D_X(u,v) + \sum_{g\notin F_r(v_0)} D_X(g,f)\right]\right| \\
&\leq \sum_{u\in B_{r+d}(v_0)\setminus B_r(v_0)} \left[\sum_{v\in B_d(u)} |D_X(u,v)| + \sum_{f\in F_d(u)} |D_X(u,f)|\right] \\
&\qquad + \sum_{g\in F_{r+d}(v_0)\setminus F_r(v_0)} \left[\sum_{v\in B_d(g)} |D_X(g,v)| + \sum_{f\in F_d(g)} |D_X(g,f)|\right] \\
&\leq |B_{r+d}(v_0) \setminus B_r(v_0)| \cdot [|B_d(v_0)| + |F_d(v_0)|] \cdot c + |F_{r+d}(v_0) \setminus F_r(v_0)| \cdot [|B_d(f_0)| + |F_d(f_0)|] \cdot c \\
&\leq c' \cdot [|B_{r+d}(v_0) \setminus B_r(v_0)| + |F_{r+d}(v_0) \setminus F_r(v_0)|],
\end{aligned}$$

where $c' = c\,[|B_d(v_0)| + |F_d(f_0)|]$. Since G is amenable and has finite maximum degree $\Delta(G)$,

$$\limsup_{r\to\infty} \frac{|B_{r+d}(v_0) \setminus B_r(v_0)| + |F_{r+d}(v_0) \setminus F_r(v_0)|}{|B_r(v_0)|} \leq \limsup_{r\to\infty} \frac{(\Delta(G)+1)|B_{r+d}(v_0) \setminus B_r(v_0)|}{|B_r(v_0)|} = 0,$$

and therefore

$$\limsup_{r\to\infty} \frac{\left|\sum_{v\in B_r(v_0)} [\mu'(v) - \mu(v)] + \sum_{f\in F_r(v_0)} [\nu'(f) - \nu(f)]\right|}{|B_r(v_0)|} = 0,$$

proving the claim. □

Theorem 3 demonstrates that (c,d)-local discharging functions provide a way to bound the density of a set X. However, as defined, the function D_X depends on the entire (possibly infinite) set X. This is not an effective strategy for us to prove anything about a discharging function. In order to build *effective* discharging functions, we will assemble one using *discharging rules*.

Informally, a discharging rule is a way to examine the local situation around a chargeable object, and then decide to exchange a certain amount of charge among nearby chargeable objects. Such a rule could, for

instance, consider which elements in $B_2(v)$ are in X, and use that information to exchange charge between v and the vertices adjacent to v, or between v and the faces incident to v. If the amount of charge exchanged depends only on the isomorphism class of the configuration $(B_2(v), B_2(v) \setminus X, B_2(v) \cap X, F_1(v))$, then this rule has a finite description, even though it is applied an infinite number of times. When several discharging rules are applied simultaneously, the discharging function D_X is defined by collecting all of the charge exchanges from all instances of the discharging rules.

Formally, a *discharging rule* is a tuple $R = (C, z, y_1, \ldots, y_t, \sigma)$ where C is a configuration, $z, y_1, \ldots, y_t$ are chargeable objects in C, and σ is a function $\sigma : \{0,1\}^{V(C)} \times \{y_1, \ldots, y_t\} \to \mathbb{R}$. We will consider the first parameter of σ to be the incidence vector corresponding to the set $X \cap V(C)$. Thus $\sigma(X \cap V(C), y_i)$ determines how much charge to exchange from y_i to z, given the realization of C For an embedding π of C into G, the rule considers $\pi^{-1}(X) \cap V(C)$ and the function σ defines that some amount of charge is exchanged from each $\pi(y_i)$ to $\pi(z)$. Thus, the rule defines a discharging function D_X^R as

$$D_X^R(a,b) = \sum_{\substack{\pi \,:\, \pi(z) = b \\ i \,:\, \pi(y_i) = a}} \sigma(\pi^{-1}(X) \cap V(C), y_i) - \sum_{\substack{\pi \,:\, \pi(z) = a \\ i \,:\, \pi(y_i) = b}} \sigma(\pi^{-1}(X) \cap V(C), y_i).$$

The above definition states that the amount of charge sent from a to b is the combination of the charge sent from a to b via all embeddings of the rule where $\pi(z) = b$ and $\pi(y_i) = a$ for some i, minus the charge sent from b to a via all embeddings of the rule where $\pi(z) = a$ and $\pi(y_i) = b$ for some i.

If $R_1, \ldots, R_m$ is a list of rules, then the discharging function D_X resulting from using these rules simultaneously is defined as $D_X(a,b) = \sum_{i=1}^{m} D_X^{R_i}(a,b)$.

We can very quickly describe the configuration C and chargeable objects $z, y_1, \ldots, y_t$ of a discharging rule. The function σ is more complicated, and in fact we do not specify it at all. For each possible element of the domain of σ, we create a variable. In the next section, we will describe how to create a linear program to assign value to these variables, thereby completely defining the discharging rules.

We now describe a few discharging rules in the hexagonal grid. The following list carefully defines each rule, but these rules can be simply described visually by Figure 3.

- V_i : Let z be a vertex, and consider the configuration on $B_i(z)$ and $F_1(z)$ and let $\{y_1, \ldots, y_t\} = F_1(z)$. Thus, this rule uses the information from $X \cap B_i(z)$ and uses that to specify how charge is exchanged to z from the faces incident to z.
- N : Let z be a vertex and consider the configuration on $F_1(z)$ that contains all vertices incident to the faces in $F_1(z)$. In the hexagonal grid, N is larger than V_2 but smaller than V_3.
- $F_{1,3}$: Let z be a face and let f_1, f_2, f_3 be three consecutive faces adjacent to z. Let y_1, y_2 be the vertices incident to both z and f_2. Consider the configuration of all vertices incident to z, f_1, f_2, f_3.
- C_1 : Let y_1 and z be adjacent vertices and consider the configuration of vertices incident to the two faces that are incident to y_1 and z.
- C_2 : Let z be a vertex, f be one of the faces incident to z, and let y_1 and y_2 be the vertices incident to f that are at distance 2 from z. Consider the configuration of vertices that are incident to f or adjacent to a vertex incident to f.
- E_1 : Let z and y_1 adjacent faces, and consider the configuration of vertices incident to z or y_1.
- E_6 : Let z be a face, $y_1, \ldots, y_6$ be the faces adjacent to z, and consider the configuration of vertices incident to z or adjacent to a vertex incident to z.

It is possible to define an infinite number of discharging rules. Note that some rules are inherently *more complex* than others, so a partial ordering can be defined on the rules. For instance, $V_1 \subset V_2 \subset N \subset V_3$,

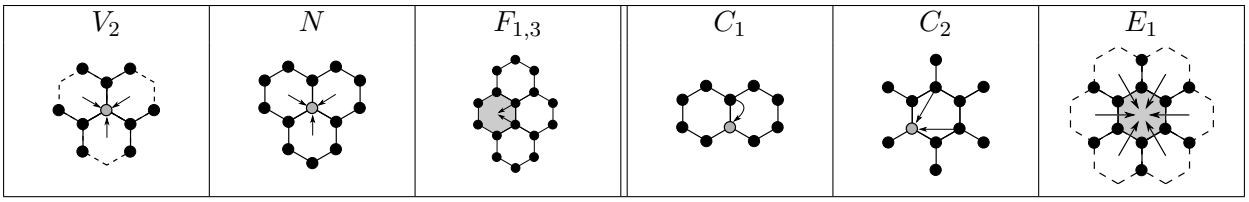

Figure 3: Examples of Rules in the Hexagonal Grid.

so N is at least as effective as V_2. We call attention to a few features of the discharging rules that should be balanced carefully in order to create the most effective rules.

Scope of Information. The larger the configuration used for the discharging rule, the more information is known about the local environment of the chargeable object receiving charge. However, as the configuration C grows, the number of realizations of the rule grows approximately as $2^{|V(C)|}$, with some loss for symmetry and for avoiding forbidden configurations.

Range of Exchange. Depending on the distance between z and the y_i's, charge can be exchanged across several distances. It may be beneficial to allow for charge to move longer distances, especially if it is possible to have large regions in G where X is much less dense than in other areas.

Dependence. For nearby chargeable objects, the configurations for different discharging rules overlap. Thus, some information is shared between the chargeable objects and that information can be used to assign value to the rule.

This step of creating a discharging argument is the step that requires the most amount of creativity and human intervention. Creating interesting and effective rules is really where the proof author has most control, and this step is absolutely crucial in determining whether a discharging proof will provide a strong lower bound. The strength of the rules must be balanced with the computational challenge of verifying their correctness, which is the topic of the next section. Armed with a set of discharging rules, we can now define the algorithmic process for assigning value to the discharging rules.

4 The Linear Program

The most difficult part of assigning value to discharging rules is verifying that objects of low charge receive enough charge to meet the goal charge while guaranteeing that objects of high charge do lot lose so much charge they drop below the goal charge. In the contrapositive, it must be impossible to construct a configuration around a chargeable object where every discharging rule is evaluated and the resulting charge violates the goal charge. Thus, we shall create a configuration C around each chargeable object (up to isomorphism) such that C contains the shape of each rule that can exchange charge to or from that object, and then generate each $\mathcal{F}$-realization of C. Every such realization determines which realizations of the discharging rules to use, and these values are combined to form a constraint in a linear program.

Recall that our goal requirement for vertices and faces are the following inequalities:

$$\mu'(v) = \mu(v) + \sum_{u \in V(G)} D_X(u, v) + \sum_{g \in F(G)} D_X(g, v) \geq w$$
$$\nu'(f) = \nu(f) + \sum_{u \in V(G)} D_X(u, f) + \sum_{g \in F(G)} D_X(g, f) \geq 0$$

Since we are using a finite list of finite-sized discharging rules, this inequality will in fact use a finite number of nonzero terms. Also, the amount of exchanged charge depends on a finite-sized local region about each chargeable object. Given a grid G and a list $R_1, \ldots, R_m$ of discharging rules, the *constraint con-*

figuration about a chargeable object x is defined as the set of faces and vertices that appear in an embedding $\pi(C)$ of a configuration $C = C(R_j)$ such that $\pi(z(R_j)) = x$ or $\pi(y_i(R_j)) = x$ for some i. Observe that the constraint configurations about two chargeable objects, x and x', are isomorphic if and only if x and x' are in orbit within G.

For example, consider the rules N and J_2 in the hexagonal grid. Since the hexagonal grid is vertex-transitive and face-transitive, we only need to consider the constraint configurations for v_0 and f_0. About v_0, there are three embeddings of N and three embeddings of J_2 such that the vertices $z(N)$ and $z(J_2)$ are mapped to v_0. Together, these embeddings form a constraint configuration about v_0 consisting of all faces in $F_2(v_0)$, and all vertices incident to a face in $F_2(v_0)$. About f_0, there are 18 embeddings of N and six embeddings of J_2 such that one of the faces $y_1(N), y_2(N), y_3(N)$ or the face $y_1(J_2)$ are mapped to f_0. Together, these embeddings form a constraint configuration about f_0 consisting of all faces in $F_1(f_0)$ and all vertices incident to a face in $F_1(f_0)$. These constraint configurations are shown in Figure 4.

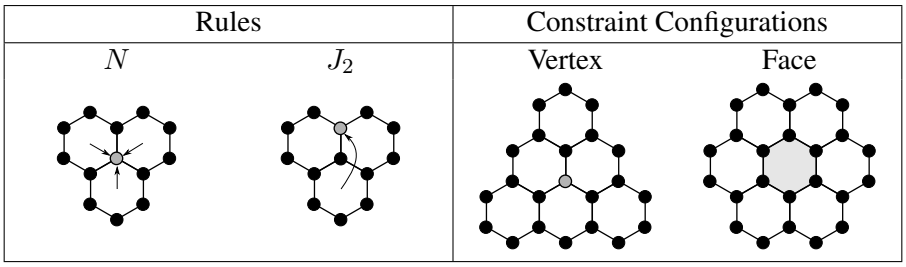

Figure 4: The rules N and J_2 and the resulting constraint configurations.

Given a constraint configuration, the way the discharging rules assign value to the charge exchange is determined exactly by the way that X intersects the vertices of this configuration. Therefore, we generate all $\mathcal{F}$-realizations of the constraint configuration. Given an $\mathcal{F}$-realization C' of our constraint configuration C, we add a constraint to our linear program.

Suppose we are using the rules $R_1, \ldots, R_k$. If C is a constraint configuration centered on a vertex v and C' is an $\mathcal{F}$-realization of C, then we enforce that $\mu'(v) \geq w$ after the discharging process is complete by adding the constraint

$$\mu(v) + \sum_{j=1}^{k} \sum_{\pi:\pi(z(R_j))=v} \sum_{i} \sigma_j(S_1(C'), y_i) - \sum_{j=1}^{k} \sum_{i,\pi:\pi(y_i(R_j))=v} \sigma_j(S_1(C'), y_i) \geq w$$

to the linear program. If C is a constraint configuration centered on a face f and C' is an $\mathcal{F}$-realization of C, then we enforce that $\nu'(f) \geq w$ after the discharging process is complete by adding the constraint

$$\nu(f) + \sum_{j=1}^{k} \sum_{\pi:\pi(z(R_j))=f} \sum_{i} \sigma_j(S_1(C'), y_i) - \sum_{j=1}^{k} \sum_{i,\pi:\pi(y_i(R_j))=f} \sigma_j(S_1(C'), y_i) \geq 0$$

to the linear program.

Observe that whenever these constraints are satisfied, the discharging argument demonstrates a lower bound of $\delta(X) \geq w$ for any $X \in \text{forb}(\mathcal{F})$. In order to produce the largest lower bound, use $\max w$ as the optimization function of the linear program.

Thus, we have a complete description of an adage proof. In summary, the three main steps are: (1) Define a set of rules $R_1, \ldots, R_k$, and generate all $\mathcal{F}$-realizations C' of their configurations, mapping the

values $\sigma_j(S_1(C'), y_i)$ to a list of variables; (2) For each constraint configuration (up to isomorphism), generate all $\mathcal{F}$-realizations and add the resulting constraint to the linear program; (3) Solve the linear program to determine the values $\sigma_j(S_1(C'), y_i)$ and the lower bound w.

These steps were implemented and executed for several sets of rules, which are shown along with their constraint configurations in Appendix A. All software and data are available online[1]. The following theorem implies Theorem 1.

Theorem 4. *Let X be an identifying code in the hexagonal grid. The adage proof using rule N demonstrates $\delta(X) \geq \frac{23}{55} \approx 0.4181818$.*

The ADAGE framework as described is not tied to any specific grid or family of forbidden configurations $\mathcal{F}$. In the next section, we discuss variations on identifying codes and summarize the adage proofs of sharp lower bounds for those variations.

5 Variations

Due to the modular development of the ADAGE framework for grids, the components for the grid and the forbidden configurations can be interchanged. This allows for adage proofs to be constructed for the hexagonal, square, and triangular grids. Several discharging rules and corresponding constraint configurations for these grids are demonstrated in Tables 2, 3, and 4. More planar grids could be implemented and used, including those that are not vertex- or face-transitive, such as the hexagon-triangle grid.

There are several variations of an identifying code, each with its own application to fault-detection in computer networks. A set $X \subset V(G)$ matches these variations if the following constraints are satisfied:

- Dominating Set: $N[v] \cap X \neq \varnothing$ for all $v \in V(G)$.
- Identifying Code: $N[v] \cap X \neq \varnothing$ and $(N[v] \cap X) \neq (N[u] \cap X)$ for all distinct $u, v \in V(G)$.
- Strong Identifying Code: $N[v] \cap X \neq \varnothing$ and $\{N[v] \cap X, N(v) \cap X\} \cap \{N[u] \cap X, N(u) \cap X\} = \varnothing$ for all distinct $u, v \in V(G)$ (see [14, 18]).
- Locating-Dominating Code: $N(v) \cap X \neq \varnothing$ for $v \notin X$, and $N(v) \cap X \neq N(u) \cap X$ for all distinct $u, v \in V(G) \setminus X$ (see [4, 13, 16, 32]).
- Open-Locating-Dominating (OLD) Code: $N(v) \cap X \neq \varnothing$ and $N(u) \cap X \neq N(v) \cap X$ for all distinct $u, v \in V(G)$ (see [22, 31]).

All of these variations are implemented in the current version of ADAGE on grids. Several collections of discharging rules were used to find adage proofs of lower bounds on these variations, and the results can be found in Table 5. We summarize the sharp bounds below, with attribution to the first authors to find such bounds. See Appenix B for lower bounds demonstrated by other rule sets.

Theorem 5 (Ben-Haim and Litsyn [3])**.** *Let X be an identifying code in the square grid. The adage proof using the rule V_2 demonstrates $\delta(X) \geq \frac{7}{20}$.*

Theorem 6 (Karpovsky, Chakrabarty, and Levitin [21])**.** *Let X be an identifying code in the triangular grid. The adage proof using the rule V_1 demonstrates $\delta(X) \geq \frac{1}{4}$.*

Theorem 7 (Honkala [13])**.** *Let X be a locating-dominating code in the hexagonal grid. The adage proof using the rule V_2 demonstrates $\delta(X) \geq \frac{1}{3}$.*

Theorem 8 (Slater [33])**.** *Let X be a locating-dominating code in the square grid. The adage proof using the rule C_1 demonstrates $\delta(X) \geq \frac{3}{10}$.*

[1] See `http://www.math.iastate.edu/dstolee/r/adage.htm` for all software and data.

Theorem 9 (Seo and Slater [31]). *Let X be an open-locating dominating code in the hexagonal grid. The adage proof using the rule V_2 demonstrates $\delta(X) \geq \frac{1}{2}$.*

Theorem 10 (Seo and Slater [31]). *Let X be an open-locating dominating code in the square grid. The adage proof using the rule C_1^+ demonstrates $\delta(X) \geq \frac{2}{5}$.*

Theorem 11 (Kincaid, Oldham, and Yu [22]). *Let X be an open-locating dominating code in the triangular grid. The adage proof using the rule C_1^+ demonstrates $\delta(X) \geq \frac{4}{13}$.*

Observe that among all variations on all three grids, the only variations that failed to find a sharp lower bound were identifying codes on the hexagonal grid, and strong identifying codes on all three grids. Likely, the strong identifying codes are more challenging because a strong identifying code is both an identifying code and an open-locating dominating code, so the optimal density is highest among all of these variations. Also, there are more forbidden configurations and this leads to fewer realizations of the discharging rules (and hence fewer variables in the linear program).

There are also variations on identifying codes that are robust against edge changes [12, 15, 17, 24, 33], or identify all sets of vertices of size at most ℓ [10, 23, 25], or consider balls of larger radius [19–21, 26, 29, 34, 35]. These variations are good candidates for future implementation.

6 Conclusions and Future Work

This first application of the ADAGE framework is successful in showing alternative proofs of existing sharp bounds [3, 16, 21, 22, 31, 33], and surpassing the human-written proofs of lower bounds on identifying codes in the hexagonal grid [5, 7, 8, 21]. The computer-automated portions of the method replace lengthy case analysis and can be more detailed than something within the reach of a human prover. However, the simple description of the discharging rules can perhaps lead to a deeper understanding of the structure and success of a discharging argument. By automating the process of assigning value to the discharging rules, a proof author can focus more on the creative process of designing rules. Thus, the most important part is to balance the strength of the rules against the size of the constraint configurations.

There are some features that will be added to the ADAGE framework in order to make the proofs more robust. The rules used so far are based entirely on the realization of the rule configuration. This leads to an exponential growth in the number of variables and constraints as the rules grow. To lower the number of variables, the rules could be clustered by families of realizations. For example, a rule could be based on the number of elements incident to a face instead of the exact arrangement of elements on the face. This is equivalent to placing equality constraints among groups of variables coming from similar realizations. Such a clustering of rules can also greatly decrease the number of distinct constraints, as several realizations of a constraint configuration will result in the same combination of variables.

Another feature is to use the discharging argument to characterize sharp examples. If the discharging proof presents a sharp lower bound on the density of a set, then we can use this to generate a class of optimal examples. Among all optimal sets, the configurations of optimal density must be those where the discharging arguments are sharp, except at a density-zero portion of the chargeable objects. Thus, it must be possible to construct arbitrarily large configurations that do not contain a forbidden configuration and the discharging rules result in charge exactly w on every internal vertex and exactly 0 on every internal face. A combinatorial generation algorithm could discover such configurations.

Acknowledgements

Thanks to Michael Ferrara, Stephen G. Hartke, Bernard Lidický, Ryan R. Martin, and Paul S. Wenger for several very helpful discussions about the discharging method and identifying codes.

References

[1] K. Appel, W. Haken, et al. Every planar map is four colorable. Part I: Discharging. *Illinois Journal of Mathematics*, 21(3):429–490, 1977.

[2] K. Appel, W. Haken, J. Koch, et al. Every planar map is four colorable. Part II: Reducibility. *Illinois Journal of Mathematics*, 21(3):491–567, 1977.

[3] Y. Ben-Haim and S. Litsyn. Exact minimum density of codes identifying vertices in the square grid. *SIAM Journal on Discrete Mathematics*, 19(1):69–82, 2005.

[4] J. Cáceres, C. Hernando, M. Mora, I. M. Pelayo, and M. L. Puertas. Locating–dominating codes: Bounds and extremal cardinalities. *Applied Mathematics and Computation*, 220:38–45, 2013.

[5] G. D. Cohen, I. Honkala, A. Lobstein, and G. Zémor. Bounds for codes identifying vertices in the hexagonal grid. *SIAM Journal on Discrete Mathematics*, 13(4):492–504, 2000.

[6] D. W. Cranston and D. B. West. A guide to the discharging method. *arXiv preprint arXiv:1306.4434*, 2013.

[7] D. W. Cranston and G. Yu. A new lower bound on the density of vertex identifying codes for the infinite hexagonal grid. *The Electronic Journal of Combinatorics*, 16(1):R113, 2009.

[8] A. Cukierman and G. Yu. New bounds on the minimum density of an identifying code for the infinite hexagonal grid. *Discrete Applied Mathematics*, 161(18):2910–2924, 2013.

[9] X. Dong, M. C. Vuran, and S. Irmak. Autonomous precision agriculture through integration of wireless underground sensor networks with center pivot irrigation systems. *Ad Hoc Networks*, 11(7):1975–1987, 2013.

[10] F. Foucaud, T. Laihonen, and A. Parreau. An improved lower bound for $(1, \leq 2)$-identifying codes in the king grid. *arXiv preprint arXiv:1111.2477*, 2011.

[11] S. G. Hartke and D. Stolee. Uniquely K_r-saturated graphs. *The Electronic Journal of Combinatorics*, 19(4):P6, 2012.

[12] I. Honkala. An optimal edge-robust identifying code in the triangular lattice. *Annals of Combinatorics*, 8(3):303–323, 2004.

[13] I. Honkala. An optimal locating-dominating set in the infinite triangular grid. *Discrete Mathematics*, 306(21):2670–2681, 2006.

[14] I. Honkala. An optimal strongly identifying code in the infinite triangular grid. *The Electronic Journal of Combinatorics*, 17(1):R91, 2010.

[15] I. Honkala, M. G. Karpovsky, and L. B. Levitin. On robust and dynamic identifying codes. *Information Theory, IEEE Transactions on*, 52(2):599–612, 2006.

[16] I. Honkala and T. Laihonen. On locating–dominating sets in infinite grids. *European Journal of Combinatorics*, 27(2):218–227, 2006.

[17] I. Honkala and T. Laihonen. On identifying codes that are robust against edge changes. *Information and Computation*, 205(7):1078–1095, 2007.

[18] I. Honkala, T. Laihonen, and S. Ranto. On strongly identifying codes. *Discrete Mathematics*, 254(1):191–205, 2002.

[19] V. Junnila. New lower bound for 2-identifying code in the square grid. *Discrete Applied Mathematics*, 161(13):2042–2051, 2013.

[20] V. Junnila and T. Laihonen. Optimal lower bound for 2-identifying code in the hexagonal grid. *arXiv preprint arXiv:1202.0670*, 2012.

[21] M. G. Karpovsky, K. Chakrabarty, and L. B. Levitin. On a new class of codes for identifying vertices in graphs. *Information Theory, IEEE Transactions on*, 44(2):599–611, 1998.

[22] R. Kincaid, A. Oldham, and G. Yu. Optimal open-locating-dominating sets in infinite triangular grids. *arXiv preprint arXiv:1403.7061*, 2014.

[23] T. Laihonen. On optimal edge-robust and vertex-robust $(1, \leq \ell)$-identifying codes. *SIAM Journal on Discrete Mathematics*, 18(4):825–834, 2005.

[24] T. Laihonen. On robust identification in the square and king grids. *Discrete Applied Mathematics*, 154(17):2499–2510, 2006.

[25] T. Laihonen. Optimal t-edge-robust r-identifying codes in the king lattice. *Graphs and Combinatorics*, 22(4):487–496, 2006.

[26] R. Martin and B. Stanton. Lower bounds for identifying codes in some infinite grids. *The Electronic Journal of Combinatorics*, 17(R122):1, 2010.

[27] A. A. Razborov. Flag algebras. *The Journal of Symbolic Logic*, 72(04):1239–1282, 2007.

[28] A. A. Razborov. Flag algebras: an interim report. In *The Mathematics of Paul Erdős II*, pages 207–232. Springer, 2013.

[29] D. L. Roberts and F. S. Roberts. Locating sensors in paths and cycles: The case of 2-identifying codes. *European Journal of Combinatorics*, 29(1):72–82, 2008.

[30] N. Robertson, D. Sanders, P. Seymour, and R. Thomas. The four-colour theorem. *Journal of Combinatorial Theory, Series B*, 70(1):2–44, 1997.

[31] S. J. Seo and P. J. Slater. Open neighborhood locating-dominating sets. *Australasian J. Combin*, 46:109–120, 2010.

[32] P. J. Slater. Locating dominating sets and locating-dominating sets. In *Graph Theory, Combinatorics and Applications: Proceedings of the Seventh Quadrennial International Conference on the Theory and Applications of Graphs*, volume 2, pages 1073–1079, 1995.

[33] P. J. Slater. Fault-tolerant locating-dominating sets. *Discrete Mathematics*, 249(1):179–189, 2002.

[34] B. Stanton. Improved bounds for r-identifying codes of the hex grid. *SIAM Journal on Discrete Mathematics*, 25(1):159–169, 2011.

[35] J. Ville and T. Laihonen. Optimality of a 2-identifying code in the hexagonal grid. In *WCC 2011-Workshop on coding and cryptography*, pages 47–56, 2011.

[36] D. B. West. *Introduction to graph theory*, volume 2. Prentice Hall Upper Saddle River, 2001.

A Discharging Rules and Constraint Configurations

Rules	Constraint Configurations
V_1 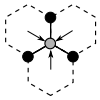	
V_2 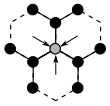	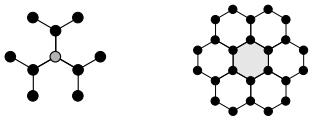
N 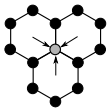	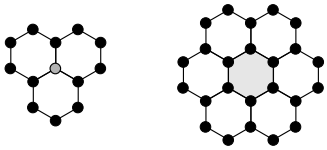
N^+ 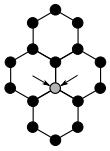	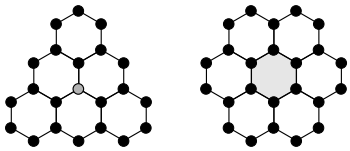
V_3	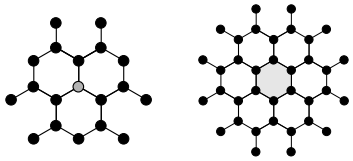
C_1 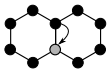	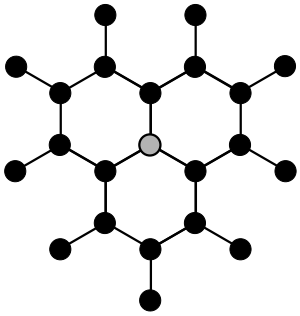
C_2^+ 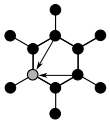	
C_3 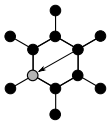	

Rules	Constraint Configurations
N 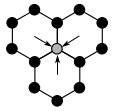	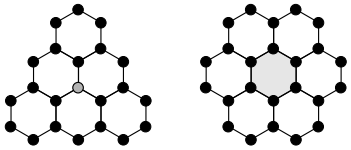
J_2 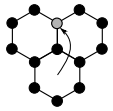	
V_3 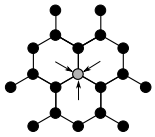	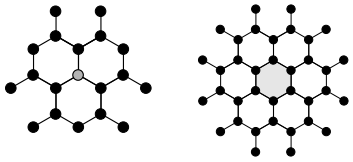
E_6 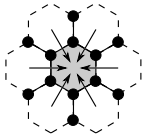	
N 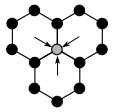	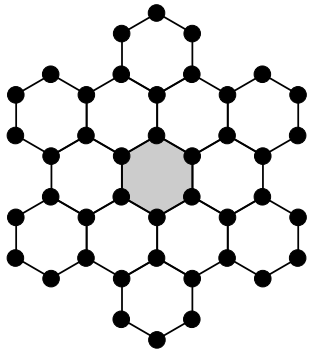
$E_{1,3}$ 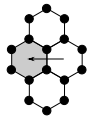	
Y_{size} 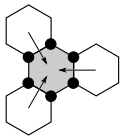	

Table 2: Various Rules and Constraint Configurations in the Hexagonal Grid.

Rules	Constraint Configurations
V_1	
N	
V_2 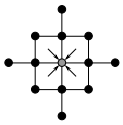	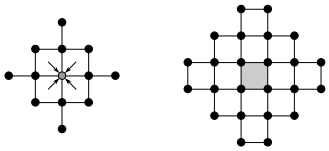
C_1	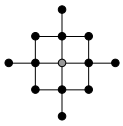
C_1^+	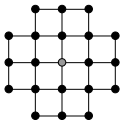
C_2 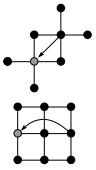	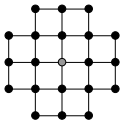
C_2^+ 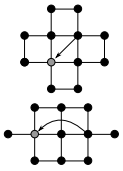	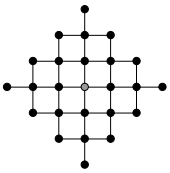

Rules	Constraint Configurations
C_1 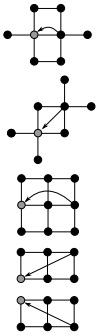	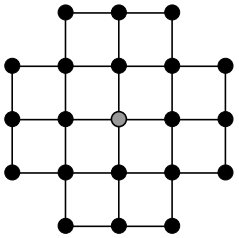
C_2	
C_3	
C_1^+ 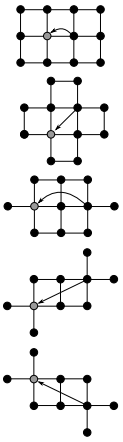	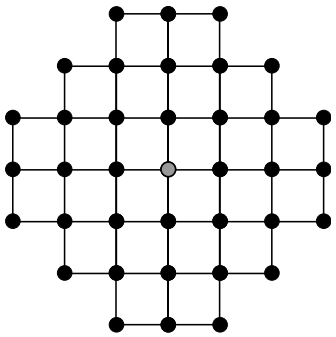
C_2^+	
C_3^+	
N 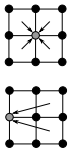	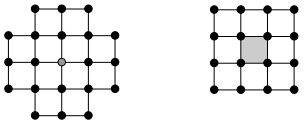
J_2	
N^+ 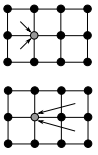	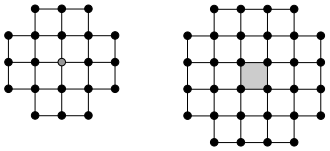
J_2^+	

Table 3: Various Rules and Constraint Configurations in the Square Grid.

Rules	Constraint Configurations
V_1	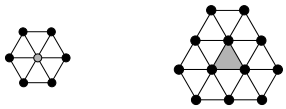
S 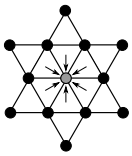	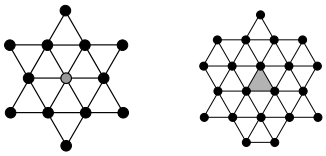
N^+ 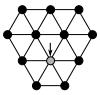	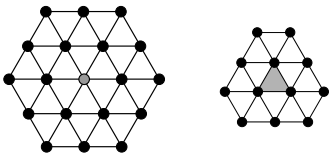
V_2 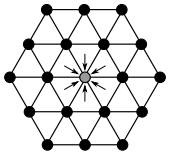	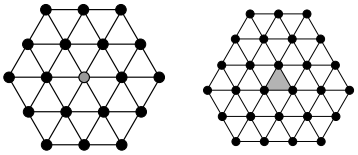
C_1 C_2 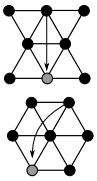	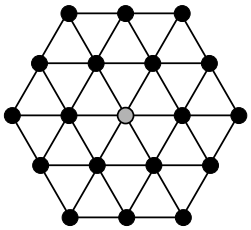
C_1^+ 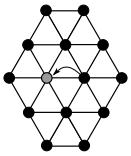 C_2^+ 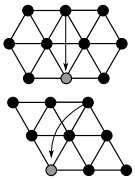	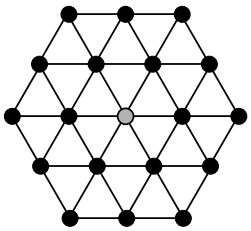

Rules	Constraint Configurations
C_1 C_2 C_3 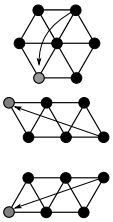	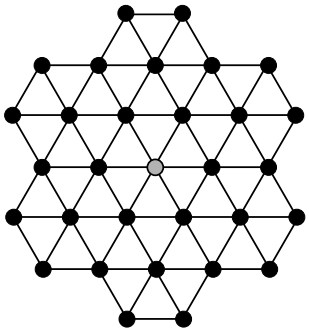
C_1^+ 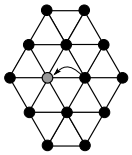 C_2^+ 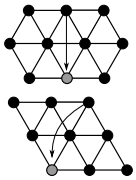 C_3^+ 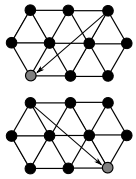	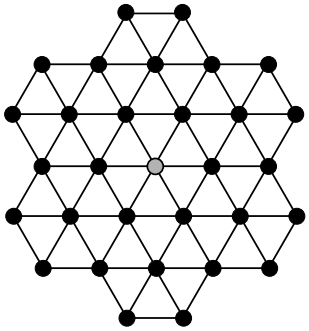
V_1 J_2	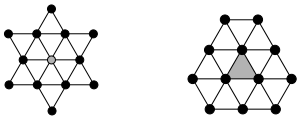
S 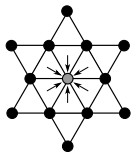 J_2^+ 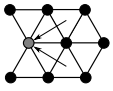	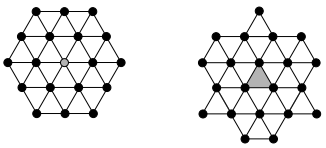

Table 4: Various Rules and Constraint Configurations in the Triangular Grid.

B Bounds on Codes Using ADAGE

Set Type	**Hexagonal Grid**		**Square Grid**		**Triangular Grid**	
Dominating Set	V_1	$\frac{1}{4} \approx 0.250000^*$	V_1	$\frac{1}{5} \approx 0.200000^*$	V_1	$\frac{1}{7} \approx 0.142857^*$
Identifying Code	V_1	$\frac{2}{5} \approx 0.400000$	V_1	$\frac{3}{10} \approx 0.300000$	V_1	$\frac{1}{4} \approx 0.250000^*$
	V_2	$\frac{33}{80} \approx 0.412500$	N	$\frac{8}{25} \approx 0.320000$	C_1^+	$\frac{1}{4} \approx 0.250000^*$
	C_1	$\frac{33}{80} \approx 0.412500$	V_2	$\frac{7}{20} \approx 0.350000^*$	C_1, C_2	$\frac{1}{4} \approx 0.250000^*$
	C_1, C_2^+	$\frac{33}{80} \approx 0.412500$	C_1	$\frac{7}{20} \approx 0.350000^*$		
	N	$\frac{23}{55} \approx 0.418182^\dagger$				
	N, J_2	$\frac{23}{55} \approx 0.418182^\dagger$				
	Upper [5]:	$\frac{3}{7} \approx 0.428571^\ddagger$	*Upper* [3]:	$\frac{7}{20} \approx 0.350000^*$	*Upper* [21]:	$\frac{1}{4} \approx 0.250000$
Strong Identifying Code	V_1	$\frac{17}{40} \approx 0.425000$	V_1	$\frac{1}{3} \approx 0.333333$	V_1	$\frac{1}{4} \approx 0.250000$
	V_2	$\frac{8}{17} \approx 0.470588$	V_2	$\approx$	S	$\frac{22}{73} \approx 0.301370$
	C_1	$\frac{8}{17} \approx 0.470588$	C_1	$\frac{22}{57} \approx 0.385964$	C_1^+	$\frac{5}{16} \approx 0.312500$
	C_1, C_2	$\frac{8}{17} \approx 0.470588$	C_1, C_2	$\frac{7}{18} \approx 0.388889$	C_1^+, C_2^+	$\frac{4}{13} \approx 0.307692$
	Upper [14]:	$\frac{1}{2} \approx 0.50000^*$	*Upper* [14]:	$\frac{2}{5} \approx 0.400000^*$	*Upper* [14]:	$\frac{6}{19} \approx 0.315789^*$
Locating-Dominating Code	V_1	$\frac{4}{13} \approx 0.307692$	V_1	$\frac{1}{4} \approx 0.250000$	V_1	$\frac{2}{11} \approx 0.181818$
	V_2	$\frac{1}{3} \approx 0.333333^*$	V_2	$\frac{3}{10} \approx 0.300000^*$	S	$\frac{9}{41} \approx 0.219512$
	C_1	$\frac{1}{3} \approx 0.333333^*$	C_1	$\frac{3}{10} \approx 0.300000^*$	C_1^+	$\frac{2}{9} \approx 0.222222$
	C_1, C_2	$\frac{1}{3} \approx 0.333333^*$	C_1, C_2	$\frac{3}{10} \approx 0.300000^*$	C_1, C_2	$\frac{12}{53} \approx 0.226415$
	Upper [16]:	$\frac{1}{3} \approx 0.333333^*$	*Upper* [33]:	$\frac{3}{10} \approx 0.300000^*$	*Upper* [13]:	$\frac{13}{57} \approx 0.228070^*$
Open-Locating-Dominating Code	V_1	$\frac{4}{9} \approx 0.444444$	V_1	$\frac{1}{3} \approx 0.333333$	V_1	$\frac{2}{9} \approx 0.222222$
	V_2	$\frac{1}{2} \approx 0.500000^*$	N	$\frac{1}{3} \approx 0.333333$	C_1, C_2	$\frac{7}{23} \approx 0.304347$
	C_1	$\frac{1}{2} \approx 0.500000^*$	C_1^+	$\frac{2}{5} \approx 0.400000^*$	C_1^+	$\frac{4}{13} \approx 0.307692^*$
	Upper [31]:	$\frac{1}{2} \approx 0.500000^*$	*Upper* [31]:	$\frac{2}{5} \approx 0.400000^*$	*Upper* [22]:	$\frac{4}{13} \approx 0.307692^*$

* Bound given is optimal lower bound on density.

† Bound given is current-best lower bound on density, but may not be optimal.

‡ Bound given is current-best upper bound on density, but may not be optimal.

Table 5: Density lower bounds for various set types in various grids, using various discharging rules.